PROCEEDINGS OF SCIENCE

Neutron and proton EDM with $N_f = 2+1$ domain-wall fermion

Eigo Shintani*
PRISMA Cluster of Excellence, Institut für Kernphysik and Helmholtz Institute Mainz, Johannes Gutenberg-Universität Mainz, D-55099 Mainz, Germany
RIKEN-BNL Research Center, Brookhaven National Laboratory, Upton, NY 11973, USA
E-mail: shintani@kph.uni-mainz.de

Thomas Blum
Physics Department, University of Connecticut, Storrs, CT 06269-3046, USA
RIKEN-BNL Research Center, Brookhaven National Laboratory, Upton, NY 11973, USA
E-mail: tblum@phys.uconn.edu

Amarjit Soni
High Energy Theory Group, Brookhaven National Laboratory, Upton, NY 11973, USA
E-mail: adlersoni@gmail.com

Taku Izubuchi
Brookhaven National Laboratory, Upton, NY 11973, USA
RIKEN-BNL Research Center, Brookhaven National Laboratory, Upton, NY 11973, USA
E-mail: izubuchi@quark.phy.bnl.gov

We report the lattice QCD calculation of nuetron (and proton) electric dipole moment (EDM) with $N_f = 2+1$ domain-wall fermion. We show the preliminary results of EDM form factor using all-mode-averaging technique, and obtain the finte EDM after extrapolation into zero momentum. We also check the excited state contamination by comparison with two different time-separations between source and sink nucleon operator. Finally we discuss the other systematic uncertainties and quark mass dependence for neutron and proton EDM.

31st International Symposium on Lattice Field Theory LATTICE 2013
July 29 âĂŞ August 3, 2013
Mainz, Germany

*Speaker.

PoS(LATTICE 2013)298

1. Introduction

Electric dipole moment (EDM) enables us to identify the CP-violating (CPV) effect of fundamental particle in the standard model (SM) and also in beyond SM (BSM). The measurement of neutron EDM (nEDM) has been attempted in experiment so far since 1960's, however there has not been any evidence of the experimental signal. The latest experimental upper bound is found to be 2.9×10^{-26} e·cm (90% CL)[1]. From the perturbative calculation for electroweak interaction, the contribution to nEDM via CPV phase in CKM matrix is extremely small [2, 3, 4] as $d_N \sim 10^{-32}$ e·cm, whose estimate is accounted by three loop order. On the other hand, the contribution from strong interaction through the θ-term is roughly $d_N/\bar{\theta} \sim 10^{-17}$ e·cm according to the chiral quark model and some effective theories. This is unnaturally small (strong CP problem).

In lattice QCD, we have several procedures to compute EDM non-perturbatively [5, 6, 7, 8, 9]. Lattice calculation including θ term is important for the estimate of hadronic contribution to EDM, and furthermore its procedure is also applicable to extension toward BSM operator. However, in θ-term, the statistical signal in Monte-Carlo calculation is extremely worse because EDM is strongly suffered from the distribution of topological charge on gauge configurations, and thus, first of all, we need accumulate much high statistics in this calculation.

In this proceedings, we present our recent study of EDM calculation using all-mode-averaging (AMA) techniques to drastically reduce the statistical error [10, 11]. To suppress the lattice artifact due to violation of chiral symmetry, we employ the domain-wall fermion (DWF) with $N_f = 2+1$ dynamical fermion. We use the same parameter sets in [10, 11]. In the computation of the exact eigenmode, we adopt the implicitly restarted Lanczos algorithm for even-odd preconditioning Hermitian DWF operator. In AMA algorithm, the approximation is set up to the truncated solver in conjugate graduate (CG) algorithm with criteria of fixed norm of residual vector. Source points for approximation are located in every 12 separation in spatial direction and 16 separation in temporal direction, and thus total number of source location is $N_G = 32$. In Table 1, one sees the other lattice parameters we have used in this proceedings.

2. Measurement of EDM form factor

The EDM form factor $F_3^{n,p}$ is defined in the matrix element,

$$\langle N(\vec{p}_1,s_1)|V_\mu^{\rm EM}|N(\vec{p}_0,s_0)\rangle_\theta = \bar{u}_N^\theta(\vec{p}_1,s_1)\Big[F_1(q^2)\gamma_\mu + F_2(q^2)\frac{\sigma_{\mu\nu}q_\nu}{2m_N} + F_3^\theta(q^2)\frac{\gamma_5\sigma_{\mu\nu}q_\nu}{2m_N} + F_A^\theta(q^2)(iq^2\gamma_\mu\gamma_5 - 2m_N q_\mu\gamma_5)\Big]u_N^\theta(\vec{p}_0,s_0), \tag{2.1}$$

where transfer momentum is defined as $q = p_1 - p_0$. We note that the first two form factors F_1, F_2 are associated with electromagnetic (EM) form factors and the last one F_A has been known as

Table 1: Parameters used in numerical calculation. *The number in the bracket is statistics using $\Delta t = 8$.

Size	L_s	mass	#configs	N_G	N_λ	$\varepsilon_{\rm AMA}$	m_π(GeV)	Δt (fm)
$24^3 \times 64$	16	0.005	751(187)*	32	400	0.003	0.33	1.37(0.91)*
$24^3 \times 64$	16	0.01	700(132)*	32	180	0.003	0.42	1.37(0.91)*

anapole form factor which is arisen from time-reversal (T) violating effect while preserving Parity symmetry. Up to the next-to-leading order of θ, we represent the form factor with three-point function, amplitude and mass [5, 6].

On the lattice, the three-point function is expanded by θ as

$$\begin{aligned} C^{\theta}_{J_\mu}(t_1,t,t_0|p_1,p_0) &= C_{J_\mu}(t_1,t,t_0|p_1,p_0) \\ &+ i\theta C^{Q}_{J_\mu}(t_1,t,t_0|p_1,p_0) + O(\theta^2), \end{aligned} \tag{2.2}$$

In the above equation, the second term constructs the three-point function multiplied with topological charge Q. We use numerically measured topological charge. Here the EM current is defined as local bilinear form $V^{\rm EM}_\mu = \bar{q}\gamma_\mu Q_c q$ with quark charge matrix $Q_c = {\rm diag}(2/3,-1/3,-1/3)$. We multiply local EM current by the renormalization factor $Z_v = 0.7178$ whose value has been already obtained from non-perturbative renormalization [12]. Note that we ignore the disconnected diagram contribution by assuming SU(3) isospin symmetry.

To compute form factor from three-point function, it is convenient to use the following ratio

$$R^i_\mu(t_1,t,t_0|p_1,p_0) = K\frac{C^i_{J_\mu}(t_1,t,t_0|p_1,p_0)}{C_G(t_1-t_0,p_1)}\left[\frac{C_L(t_1-t,p_0)C_G(t-t_0,p_1)C_L(t_1-t_0,p_1)}{C_L(t_1-t,p_1)C_G(t-t_0,p_0)C_L(t_1-t_0,p_0)}\right]^{1/2} \tag{2.3}$$

with $K = \sqrt{(E_N(\vec{p}_1)+m_N)(E_N(\vec{p}_0)+m_N)/E_N(\vec{p}_1)E_N(\vec{p}_0)}$, as used in [13]. $E_N(p)$ means the nucleon energy in momentum p. The nucleon two-point function with smeared-source/smeared-sink is $C_G(t,p)$ and smeared-source/local-sink is $C_L(t,p)$ in momentum p at time-slice t. Next, we insert the explicit form of nucleon spinor matrix as shown in [5], in which CP-odd phase factor $\alpha_N(\theta)$ induced by θ-term appears in exponent proportional to γ_5. Since this phase leads to $\alpha_N(\theta) = \theta\alpha_N + O(\theta^3)$, taking the trace of spinor after multiplication of γ_5 for the nucleon two-point function, α_N is given as

$${\rm tr}\Big[\gamma_5 C^Q_{L/G}(t,p)\Big] = \overline{Z}_{L/G}(p)Z_G(p)\frac{2m_N}{E_N}\alpha_N\big(e^{-E_N t} + (-)^b e^{-E_N(L_t-t)}\big) + O(e^{-E_{N^*}}), \tag{2.4}$$

with the normalization factor $Z_{L/G}$ for local (L) or Gauss smearing (G) function. The parameter b indicates the boundary condition in temporal direction with L_t size; $b=0$ is periodic case and $b=1$ is anti-periodic case.

Using the leading order of $\alpha_N(\theta)$ obtained from Eq.(2.4), and therefore comparing the leading order and the next-to-leading order of θ, we directly obtain the formula of leading order $\mathscr{R}_\mu(\vec{p}_1,\vec{p}_0)$ and the next-to-leading order $\mathscr{R}^Q_\mu(\vec{p}_1,\vec{p}_0)$. Hereafter we set up to $\vec{p}_0 = \vec{p}$ and $\vec{p}_1 = 0$ (and $E_N(\vec{p}_0) = E_N$, $E_N(\vec{p}_1) = m_N$), and thus we have

$$\mathscr{R}_\mu(0,\vec{p}) = \frac{1+\gamma_4}{2}\Big[F_1(q^2)\gamma_\mu + F_2(q^2)\frac{\sigma_{\mu\nu}q_\nu}{2m_N}\Big]\frac{ip\cdot\gamma+m_N}{2E_N}, \tag{2.5}$$

$$\begin{aligned} \mathscr{R}^Q_\mu(0,\vec{p}) &= \frac{\alpha_N}{2}\gamma_5\Big[F_1(q^2)\gamma_\mu + F_2(q^2)\frac{\sigma_{\mu\nu}q_\nu}{2m_N}\Big]\frac{ip\cdot\gamma+m_N}{2E_N} \\ &+ \frac{1+\gamma_4}{2}\Big[F_1(q^2)\gamma_\mu + F_2(q^2)\frac{\sigma_{\mu\nu}q_\nu}{2m_N}\Big]\frac{\alpha m_N}{2E_N}\gamma_5 \\ &+ \frac{1+\gamma_4}{2}\Big[F_3(q^2)\frac{\gamma_5\sigma_{\mu\nu}q_\nu}{2m_N} + F_A(q^2)\Big(iq^2\gamma_\mu\gamma_5 - 2m_N q_\mu\gamma_5\Big)\Big]\frac{ip\cdot\gamma+m_N}{2E_N}. \end{aligned} \tag{2.6}$$

Following the above formula, to extract F_3 term from the second equation, we need to subtract the F_1 and F_2 terms obtained from the first equation.

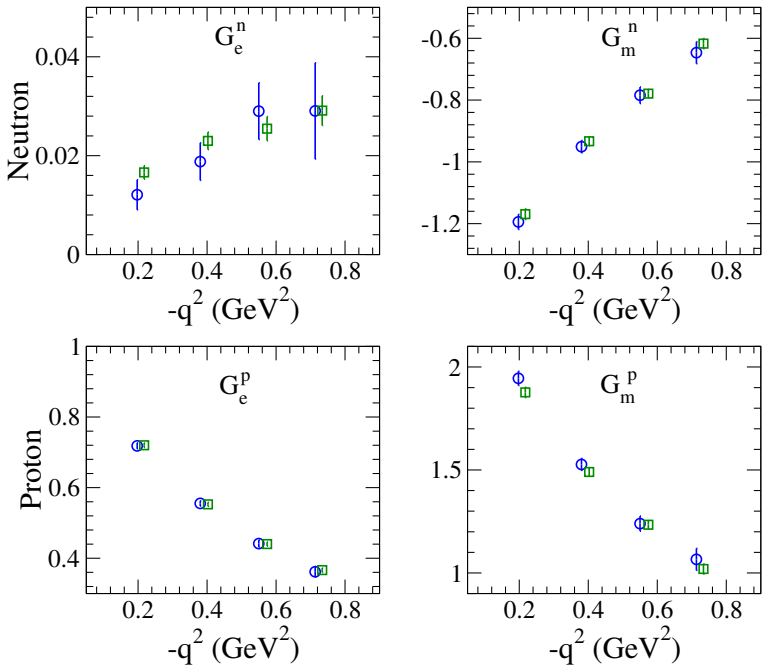

Figure 1: The q^2 dependence of Sach form factor with $\Delta t = 12$ (circle) and $\Delta t = 8$ (square) at $m = 0.005$.

3. Numerical results

First, we show the EM form factor F_1, F_2 obtained from Eq.(2.6). On this ensemble, we achieve more improvement of statistical error of these observables by using AMA. The precise measurement of EM form factor is necessary to subtract it from three-point function. Figure 1 shows the comparison of EM form factor with two time-separations, $\Delta t = 12$ and $\Delta t = 8$. These are Sach form factor, which are combination of F_1 and F_2 as $G_e(q^2) = F_1(q^2) - \frac{q^2}{4m_N}F_2(q^2)$, $G_m(q^2) = F_1(q^2) + F_2(q^2)$. One sees that, compared to long time-separation ($\Delta t = 12$), the short time-separation ($\Delta t = 8$) has a good precision which is improved as 60%–70%, especially for G_e^n. we have factor 3 improvement. The total statistical error is less than 10% accuracy.

Next, we show the fitting result of α_N obtained from $\mathcal{O}(\theta)$ term of two point function Eq.(2.4) in table 2. This indicates that the extracted results is not relied on the nucleon momentum and smearing function as expected. The precision is also around 10%–20% even if there is finite momentum, and thus it turns out that AMA works well for CP-odd observable. We notice, however, there is no appearent dependence on quark mass m, in contrast with expectation that CP-odd observable supresses approaching to the chiral limit. This may be because the quark mass is relatively large for observing such behavior and also the large statistical error.

Since the EDM form factor is extracted from three-point function from subtraction of the term proportional to α_N multiplied with EM form factor, it is important to figure out which piece is the dominant contribution. Here we decompose F_3 to two pieces,

$$F_3 = F_Q + F_\alpha. \tag{3.1}$$

Table 2: Table of fitting results of nucleon mass and CP-odd phase factor of nucleon propagator at four different momenta in $m = 0.005$. Nucleon energy is a measured value with Gaussian smeared sink operator. The subscripts "pt" and "gs" denote the function of sink operator in point type and Gaussian smeared type respectively.

$\vec{p}^2$(GeV^2)	E_N(GeV)	$\alpha_{N\,\mathrm{pt}}$	$\alpha_{N\,\mathrm{gs}}$
0.000	1.1375(24)	-0.322(41)	-0.323(35)
0.205	1.2228(27)	-0.296(38)	-0.345(40)
0.410	1.3064(34)	-0.314(49)	-0.349(46)
0.615	1.3879(51)	-0.324(70)	-0.304(53)
0.821	1.4640(90)	-0.449(204)	-0.482(154)

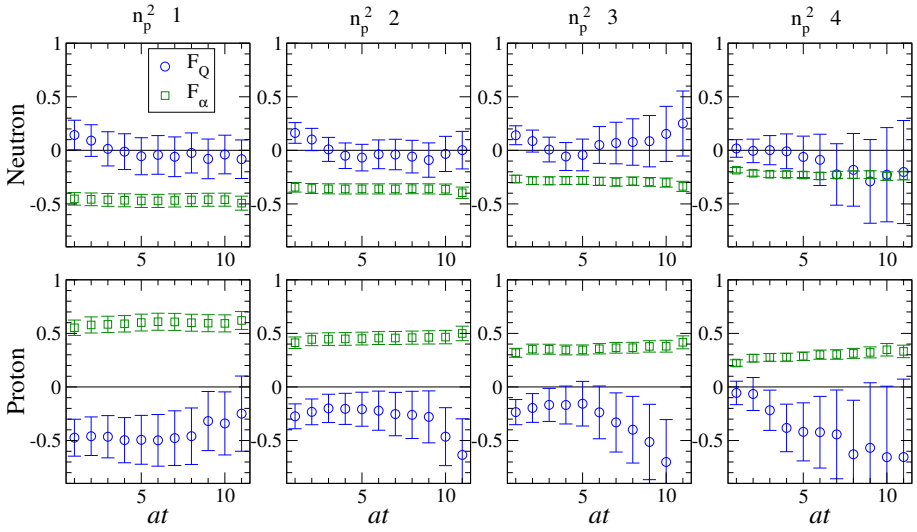

Figure 2: Time dependence of the two divided pieces of EDM form factor into F_Q and a subtraction term F_α. From left to right panels shown are the results at different insertion of momenta. Upper panel is result for neutron and the bottom is result for proton at $m = 0.005$. Here we use the three-point function of $\mu = t$ EM current.

F_Q consists of θ-NLO three-point function, and F_α contains the subtraction term F_α. From Figure 2, one sees that F_α is high precision, whose statistical error is around 10%, otherwise F_Q has rather large fluctuation whose statistical error is more than 50%. This indicates that the signal of F_3 almost relies on the accuracy and stability of the three-point function (F_Q).

To confirm the contribution of excited state contamination, we compare different time-separation Δt with $\Delta = 12$ and $\Delta t = 8$ in Figure 3. One sees that the plateau region is almost overlapping within 1 σ statistical error, and also small Δt has even better signal than $\Delta = 12$. Therefore the contamination of excited state (for instance parity partner of nucleon) is almost negligible in this range. Hereafter we only use the result of $\Delta t = 8$ with fitting region $[3,5]$.

In figure 4 we plot EDM obtained in this study and other lattice result including dynamical fermions. We extrapolate EDM form factor with linear function of $-q^2$, and to estimate the sys-

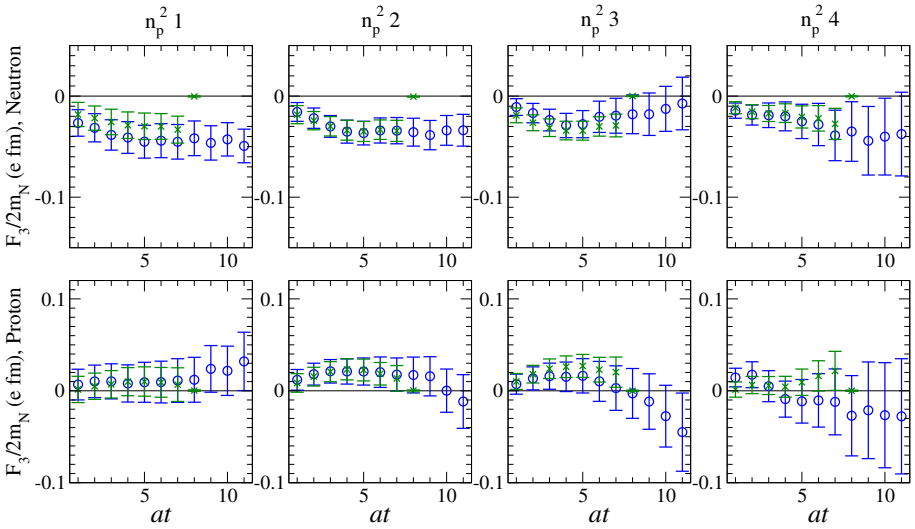

Figure 3: The comparison of the normalized EDM form factor $F_3/2m_N$ (e·fm) with different $\Delta t = 12$ (circle) and $\Delta t = 8$ (cross) for neutron (top) and proton (bottom) in $m = 0.005$ at several momenta. This is result using $\mu = t$.

tematic uncertainties for fitting function, we compare two different fitting range for $-q^2$, in which this is four points with the largest $-q^2$ or three points without the largest one. We add such systematic uncertainties into Figure 4 and show the total error. We obtain a finite neutron EDM value in the lightest quark mass, and this precision is more than 60% uncertainties remaining. In the total error, the statistical error is almost dominated, and it turns out that the reduction of statistical noise in EDM is important. For mass-dependence, as well as α_N, EDM is not suffered from the suppression as quark mass is decreased. It will be same reason as not good distribution of topological charge and response to quark mass is small. The magnitude in lattice QCD is roughly order 10 times larger than several model calculation (see [14] and reference therein), although the error is still large. Keeping highly precise calculation is more important task to compare with model prediction.

4. Summary

In this proceedings we present the recent study of EDM calculation in lattice QCD. AMA algorithm is working well even in CP-odd observable. We have good signal of EDM form factor from subtraction of EM form factor to three-point function at $\mathcal{O}(\theta)$, and we obtain the finite value of EDM after extrapolation to zero momentum limit. Currently the statistical error is still dominant for nucleon EDM, and it means that AMA provides much benefit for the error reduction of this observable. EDM calculation in physical points is next project to reach 10% precision of total error for nucleon EDM in the near future.

Numerical calculations were performed using the RICC at RIKEN and the Ds cluster at FNAL. This work was supported by the Japanese Ministry of Education Grant-in-Aid, Nos. 22540301 (TI), 23105714 (ES), 23105715 (TI) and U.S. DOE grants DE-AC02-98CH10886 (TI) and DE-

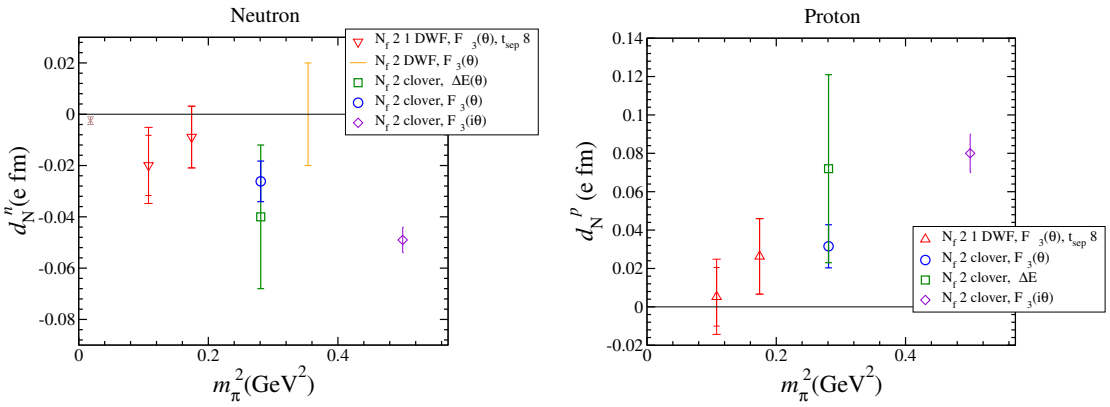

Figure 4: Summary plot of EDM for neutron (top) and proton (bottom) as a function of pion mass squared with full QCD calculation in the present analysis and other method and fermion action. Upper triangles shows our results including total error. The smaller error denotes the statistical error. The cross symbol denotes the range of model calculation based on the baryon chiral perturbation theory.

FG02-92ER40716 (TB). We also thank BNL, the RIKEN BNL Research Center, and USQCD for providing resources necessary for completion of this work.

References

[1] C. A. Baker, D. D. Doyle, P. Geltenbort, K. Green, M. G. D. van der Grinten, P. G. Harris, P. Iaydjiev and S. N. Ivanov *et al.*, Phys. Rev. Lett. **97**, 131801 (2006).

[2] I. B. Khriplovich and A. R. Zhitnitsky, Phys. Lett. B **109**, 490 (1982).

[3] I. B. Khriplovich, Phys. Lett. B **173**, 193 (1986) [Sov. J. Nucl. Phys. **44**, 659 (1986)] [Yad. Fiz. **44**, 1019 (1986)].

[4] A. Czarnecki and B. Krause, Phys. Rev. Lett. **78**, 4339 (1997).

[5] E. Shintani, *et al.*, Phys. Rev. D **72**, 014504 (2005).

[6] F. Berruto, T. Blum, K. Orginos and A. Soni, Phys. Rev. D **73**, 054509 (2006).

[7] E. Shintani, *et al.*, Phys. Rev. D **75**, 034507 (2007).

[8] E. Shintani, S. Aoki and Y. Kuramashi, Phys. Rev. D **78**, 014503 (2008).

[9] R. Horsley, T. Izubuchi, Y. Nakamura, D. Pleiter, P. E. L. Rakow, G. Schierholz and J. Zanotti, arXiv:0808.1428 [hep-lat].

[10] T. Blum, T. Izubuchi and E. Shintani, Phys. Rev. D **88**, 094503 (2013).

[11] T. Blum, T. Izubuchi and E. Shintani, PoS LATTICE **2012**, 262 (2012) [arXiv:1212.5542].

[12] Y. Aoki *et al.* [RBC and UKQCD Collaborations], Phys. Rev. D **83**, 074508 (2011).

[13] T. Yamazaki, Y. Aoki, T. Blum, H. -W. Lin, S. Ohta, S. Sasaki, R. Tweedie and J. Zanotti, Phys. Rev. D **79** (2009) 114505 [arXiv:0904.2039 [hep-lat]].

[14] T. Fukuyama, Int. J. Mod. Phys. A **27**, 1230015 (2012).